Electrochemistry of Graphene Flake Electrodes: Edge and Basal Plane Effect for Biosensing

Feifei Zhang[1,*], Lin Lu[2], Min Yang[1], Cuili Gao[1], Zonghua Wang[1,*]

[1] College of Chemistry and Chemical Engineering, Collaborative Innovation Center for Marine Biomass Fiber Materials and Textiles, Laboratory of Fiber Materials and Modern Textile, The Growing Base for State Key Laboratory, Shandong Sino-Japanese Center for Collaborative Research of Carbon Nanomaterials, Qingdao University, Qingdao 266071, China
[2] Zibo normal college, Zibo, Shandong 255200, China
[*]E-mail: wangzonghua@qdu.edu.cn, zhangfeifei00921@163.com

In order to study the properties of the graphene basal plane and edge specifically, the graphene flakes (GFs) were selectively masking with a non-conducting polymer to access the basal plane and edge only. An electro-exfoliation process was used to introduce functional groups on the surface of GFs basal plane and edge electrodes. The morphologies, structure defects, functional groups and surface states of the electrodes were studied by SEM, Raman and XPS. Depending on the electrochemical species (Fe^{3+}, UA and AA) used, we found that the GFs basal plane and edge carbon atoms could play a different role in electrochemical sensors. Furthermore, the oxygen groups induced in the electrodes, were also influenced the electrochemical properties of the GFs electrodes.

1. INTRODUCTION

Graphene has been applied to modified electrodes in various systems, such as chemical-sensors, biosensors, supercapacitors and batteries[1-4]. Graphene derivatives, including pristine graphene, graphene oxide (GO), chemically reduced GO (rGO)[5] and N-doped graphene[6] have generated much attention due to their promising applications in biosensing and detection of biomolecules such as hemin, DNA, urea and dopamine[7-11]. Previous researches have assumed that the attractive electrochemical activity and electron-transfer rate are due to the surface defects and functional groups load on the basal plane and edge.[12] It has been reported, the electron transfer of
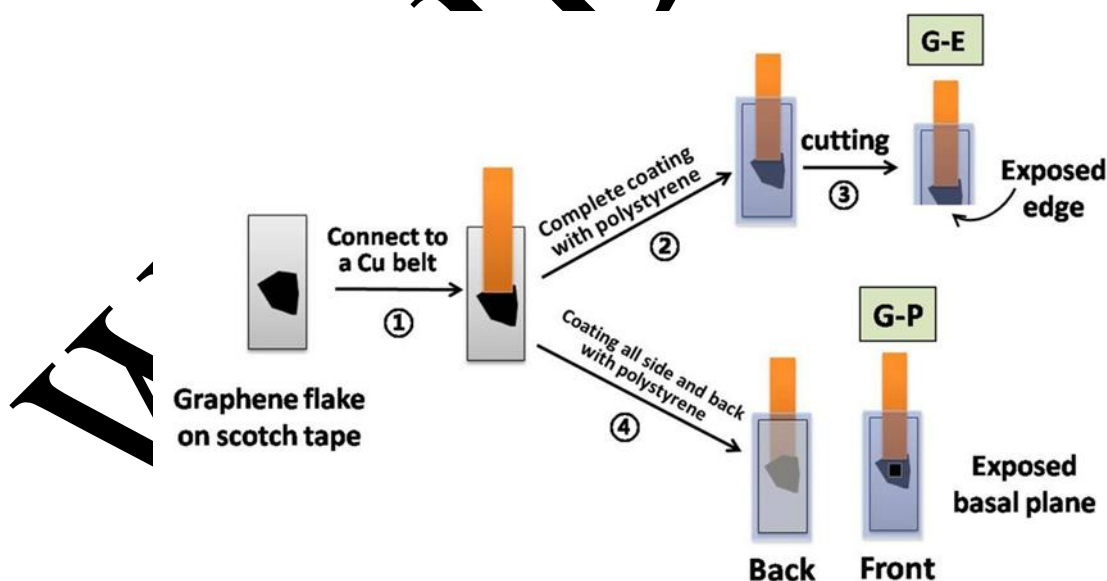
graphene happens on the edge atoms of the graphene.[13] However, no obviously result was got because of difficulties in distinguishing graphene surface atom from its edge.

This situation was further complicated by oxygen functional groups, often reacted by chemical or electrochemical oxidation of the graphene. For example, the question of whether the influence of the oxygen groups is positive or negative. Chou and co-workers reported that the carboxylic groups of single-walled carbon nanotubes were the reason for increasing the electron transfer rate constant of ferro/ferricyanide.[14] However, Ji and co-workers presented that during the increases of oxygen groups within graphite microparticles, heterogeneous electron transfer between the graphite and ferro/ferricyanide decreases.[15] The adsorption and desorption of molecules takes place in the electrochemical reaction and after the reaction, also influence the electron transfer rate.[12]

In this work, in order to study the electrochemistry of the graphene basal plane and edge specifically, we firstly used scotch tape repeatedly peeling flakes of highly oriented pyrolytic graphite (HOPG) to get the multilayer graphene flakes (GFs) fixing on the scotch tape, followed by selectively masking regions of the graphene flake with a non-conducting polymer coating (e.g. polystyrene, PS) such that the electrolyte has access the basal plane and edge only. And various electro-chemical probes, including $K_3[Fe(CN)_6]$, uric acid (UA) and ascorbic acid (AA) with specific electrochemical sensitivities to various surface states of an electrode,[15-18] were then used to detect the electrochemical propertes of the basal plane and edge atoms.

2. EXPERIMENTAL

2.1. Fabrication of edge (G-E) and basal plane (G-P) electrodes from graphene flake

Figure 1. Schematic representation of the preparation procedure of graphene electrodes with the only edge (G-E) or basal plane (G-P) carbon atoms accessible to electrolyte.

Fig. 1 shows a schematic representation of the procedure for the G-E and G-P electrodes from the GF (the thickness was measured by SEM). To start with, GFs were fixed to a copper belt (step 1)

with silver epoxy. The graphene flake edge electrode with only the edge exposed (named as G-E electrode) was prepared by coating the copper-belt-supported GF with a PS solution (10 wt% in toluene) ,and then drying at 50 °C in air (step 2), partially cutting off the free end of the polymer-wrapped GF (step 3). The access of electrolytes to the inner wall of the GF can be limited by its hydrophobicity. [9] And, the graphene electrode with the basal plane exposed (named as G-P electrode) was prepared by covering the graphene flake with a small piece of square steel (2 mm*2 mm*10 mm) firstly, then coating the all sides and back of the copper-belt-supported GF covered with the steel by the PS solution, drying at 50 °C (step 4), finally remove the steel to expose the basal plane of graphene electrode.

2.2. Electrochemical oxidation of graphene edge and basal plane electrodes

Preparation of the graphene electrodes with oxygen-containing surface functionalities (named as O x min-G-E and O y min-G-P) was operated by polarized scanning of G-E and G-P electrodes at 1.8 V in 0.1 M phosphate-buffered saline solution (PBS, pH 6.5) for different time (x and y = 3, 10, 30 min); Then they were cyclic scanned in H_2SO_4 (0.5 M) until get a stable cyclic voltammogram.

2.3. Structural and electrochemical characterization

Morphology and structure of the electrodes were characterized using, scanning electron microscopy (SEM, JEOL JSM-7001F). X-ray photoelectron spectroscopic (XPS) measurements were made on a PHI Quantera SXM (ULVAC-PHI) using monochromatic Al Kα radiation. Raman spectroscopy data were collected at room temperature using a Micro-Raman spectrometer (Nikon) with 532 nm laser source.
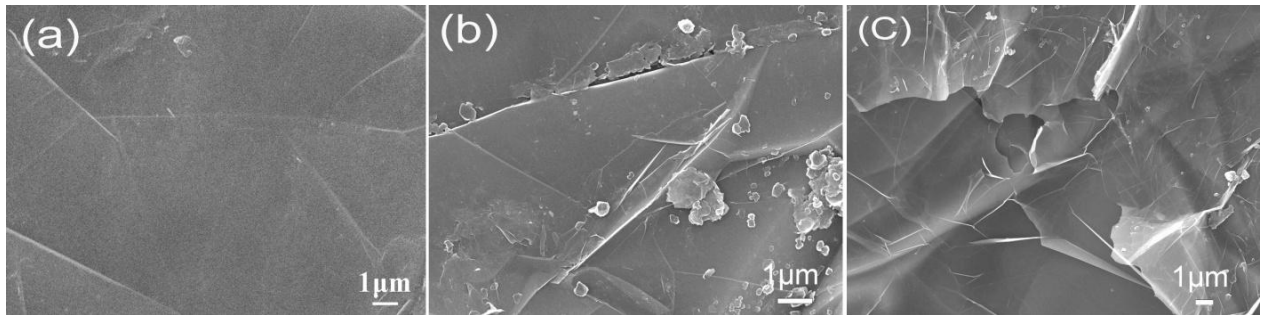
Electrochemical measurements were performed by using a BioLogic EC-Lab (VSP-300) with a three-electrodes configuration. The as-prepared G-E, G-P, O x min-G-E and O y min-G-P electrodes were used as the working electrode. The platinum wire and the saturated calomel electrode (SCE) were used as the counter electrode and the reference electrode, respectively. All potentials used were biased versus SCE.
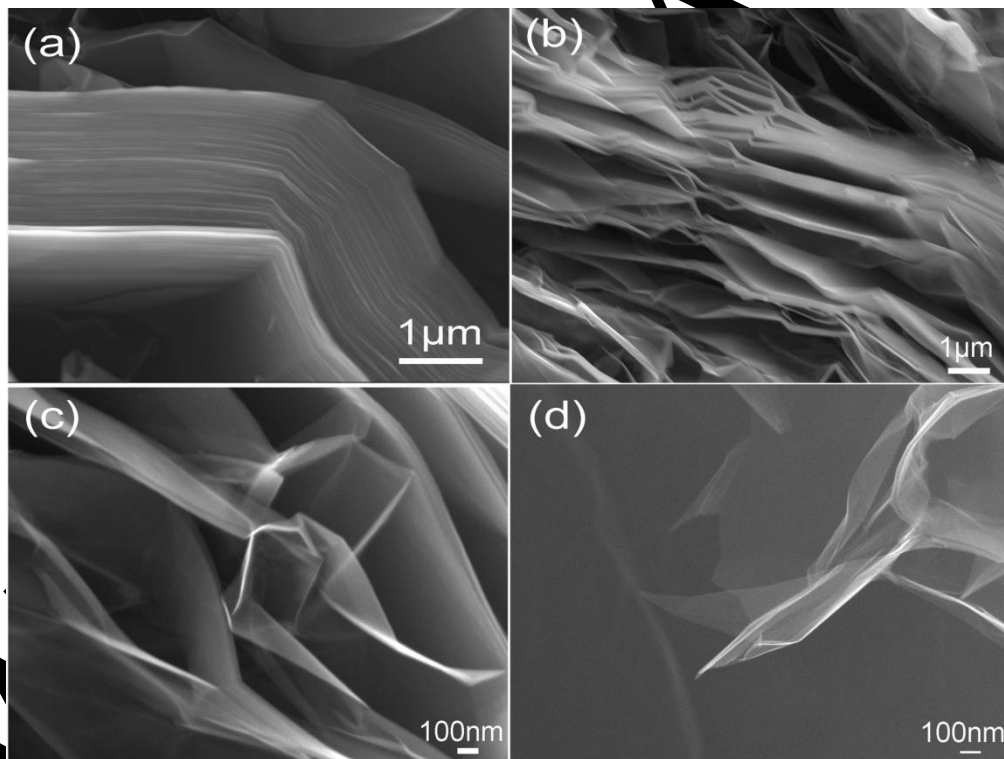
3. RESULTS AND DISCUSSION

3.1. Characterizations

Surface morphology of G-P and G-E with different oxidation times was characterized by SEM. As shown in Fig. 2a, the freshly peeled surface of graphene flakes is smooth with little wrinkles and edge planes. In Fig. 2b, after 3 min electrochemical oxidation of the graphene basal plane (O 3 min-G-P), a little structure defects caused by tiny bubbles were observed on graphene flake surface, indicating an intercalation of the solvent into graphene flake edges. It has been reported that the intercalation of electrolyte and water into graphite layers can occurred subsurface gas evolution.[17] The grain boundaries, step defects and edge sites have been reported be preferentially etched during the intercalation process, and then yields gas production from these sites.[18] And some small size single

layer or few layers graphene (several hundred nanometers) were exfoliated in the oxidized process, which was also proved by the Raman results in Fig. 4. After a long time oxidation of 30 minutes, there is a significant change observed in the surface structure of the grapheme basal plane (Fig. 2c). Most of the surface was deeply exfoliated to big size graphene flakes. And, some curved single layer or few layers graphene with size bigger than 10 micro meters was observed.
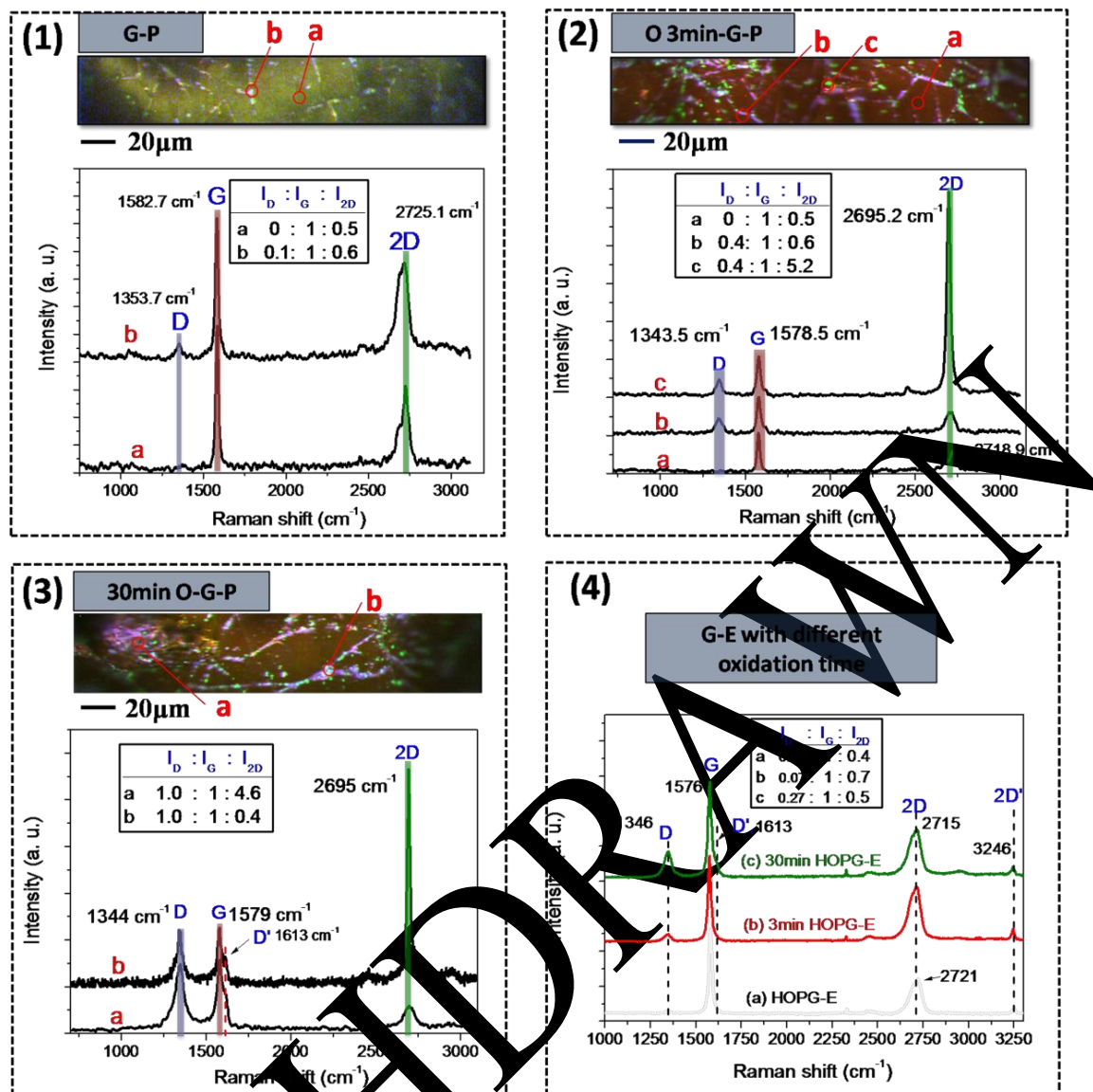

Figure 2. SEM images of the surface of (a) G-P, (b) O 3 min-G-P, and (c) O 30 min-G-P electrodes

Figure 3. SEM images of the surface of (a) G-E, (b) O 3 min-G-E, (c) O 10 min-G-E, and (d) O 30 min-G-E electrodes

SEM images of G-E electrodes in different oxidation time (0, 3, 10, 30 min) were shown in Fig. 3. Most of the surface carbon exposed to the electrolyte is edge atom (Figure 3a). Fig. 3b-d showed a typical exfoliation process of the same sample at different times.

Figure 4. Raman spectroscopy and imaging of 1) G-P, 2) O 3 min-G-P, 3) O 30 min-G-P electrodes and spectroscopy of 4) G-E with different oxidation time.

The exfoliation is easily visible by SEM after a few minutes (Fig. 3b). The graphite sheets swell because of gas formation, yielding structures like open books; the foam likes structure is instead observed. The sample volume was highly increased, much larger than the original volume. For the oxidation of G-E electrode, the thickness of O-G-E electrode increased quickly. After the oxidation of more than one hour, a large amount of materials was released in solution, resulting in a dark solution.
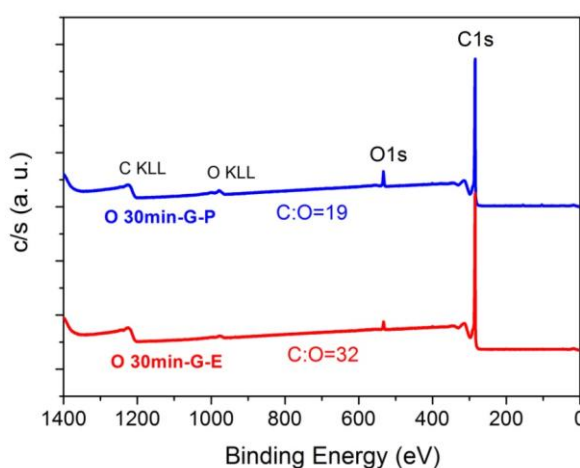
The vibration modes of molecules can be characterized by Raman spectroscopy, while the probing of a small volume can be performed with Micro-Raman spectroscopy that combines a confocal microscope and the spectroscopy system [19]. Raman spectroscopy and imaging was used as an effective tool to identify the number of graphene layers, and to probe structural and electronic characteristics of graphite materials, providing significant information on the defects (D band at ~ 1350 cm^{-1}), in-plane vibration of sp2 carbon atoms (G band at ~1580 cm^{-1}) and the stacking order (2D band at ~2670 cm^{-1}) [20].

Raman spectroscopy and imaging of G-P and G-E electrodes at different oxidation times are shown in Fig. 4. For the imaging maps, the intensity of D, G and 2D bands are colored as purple, red and green, respectively. Typical Raman spectroscopies of GF are observed at 1582.7 cm^{-1} for G band and 2725.1 cm^{-1} for 2D band in Fig. 4(1). Most of the original GF sheet surface has no defect, although a little D band at 1582.7 cm^{-1} appears, which may arise from the edge-plane defect on the surface. After electrochemical oxidization for 3 min in 0.1 M of PBS, the imaging of electrode surface undergoes a marked change in color. Especially, many green color areas appear, indicating the increase of 2D band intensity in these areas (Fig. 4(2)). For the Micro Raman spectroscopies of points b and c, some defects ($I_D/I_G = 0.4$) were introduced into the surface along the "cracks", indicating that the edge-plane atoms are easily oxidized. The intensity ratio of I_{2D}/I_G is ~5 and there is ~20 cm^{-1} blue-shift of the 2D band at point c, confirming the presence of some small single layer graphene. In the Raman spectroscopy of basal plane, O 3 min-G-P electrode shows similar phenomena with G-P, meaning that the basal plane atoms are not oxidized after a short time reaction. In the situation of O 30 min-G-P electrode (Fig. 4(3)), some defects were introduced into the basal plane after long time oxidation, with the intensity ratio of $I_D/I_G \approx 1$. A big D' band (1613 cm^{-1}) intensity was found, which also indicates the presence of defect. In addition, some of larger sized single layer and few layers graphene with defect were observed from electrochemical exfoliation. Raman spectroscopies of G-E electrodes with the oxidation for different times are shown in Fig. 4(4).
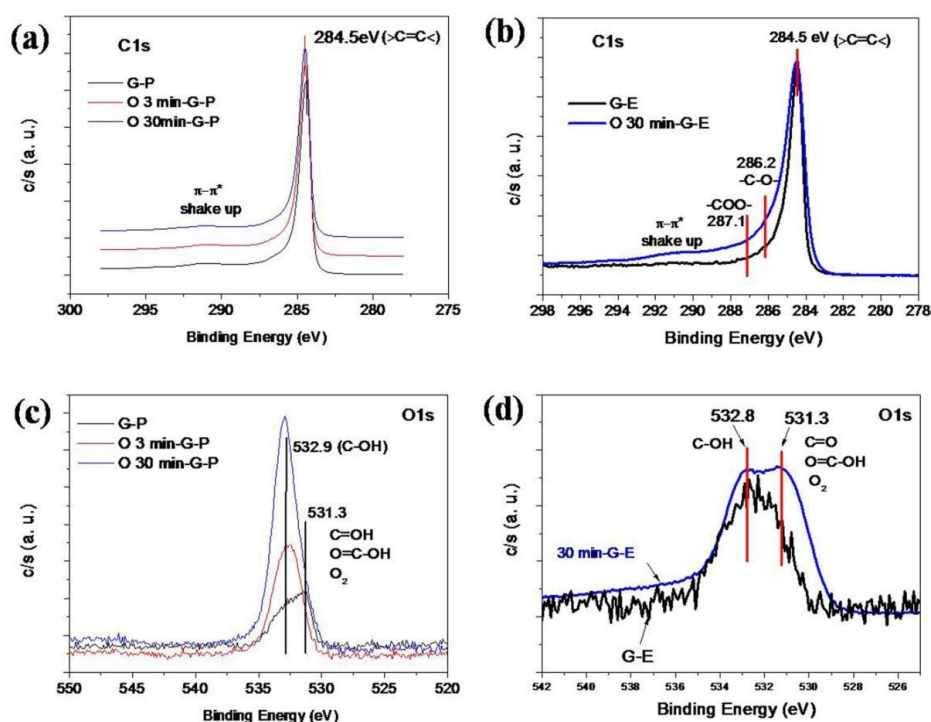
With the increase of oxidation time, the I_D/I_G intensity ratio increase from 0.07 for 3 min-oxidation to 0.27 for 30 min-oxidation. A weak band at ~3246 cm^{-1} called 2D' band, is an overtone of D' (1613 cm^{-1}) mode. In the electrochemical oxidation process, the introduction of oxygen containing groups rise defect band in Raman spectroscopy. Compared to the I_D/I_G intensity ratios of O-G-P and O-G-E electrodes, the defect content in O-G-P electrode is much larger than O-G-E electrode under the same oxidation time, which may be ascribed to the oxidation and exfoliation effects on the electrode surface simultaneously. Due to the layered structure of G-E electrode, the exfoliation effect is a little larger than oxidation effect. However, the G-P electrode only expose the basal plane surface out to the electrolyte, and the intercalation of the ions and exfoliation of the gas are much harder than the layered sidewall. Thus, the oxidation reaction may be much easier to occur, when compared to the exfoliation process.

To determine the elemental composition, chemical and electronic states of elements on the graphene electrodes surface, XPS was applied in this study. As known, the surface chemistry of modified electrodes can affect the electrochemical processes, such as the adsorption or chelation effects arising from the surface charge [21]. Fig. 5 shows the wide spectra for O 30 min-G-P and O 30 min-G-E electrodes. By calculating the signal intensities of C1s and O1s, the ratios of C: O were respectively calculated to be 19 and 32 for O 30 min-G-P and O 30 min-G-E electrode, consisting with the results from Raman experiments. After the electrochemical oxidation for 30 min, the defect caused by the introduction of oxygen groups on the G-P electrode is much more than the G-E electrode.

Figure 5. The XPS wide spectra of O 30 min-G-P and O 30 min-G-E electrodes.

Figure 6. XPS high resolution C1s spectra of G-P (a), G-E (b) and O1s spectra of G-P (c), G-E (d) with electrochemical oxidation for different time.

For the G-P electrodes at different oxidation time, high-resolution C1s and O1s of XPS spectra are shown in Fig. 6a and b. For the C1s spectra, the peaks at 284.5 eV and 291.0 eV correspond to the sp^2 hybridized graphitic carbon and the π-π^* structure, respectively. After the oxidation for 3 min and 30 min, there is no obvious change in the C1s spectra of O-G-P electrodes. For the O1s spectra, the peak at 532.9 eV corresponds to the contribution from C–OH groups and the peak at 531.3 eV corresponds to the C=O and O=C–OH groups or some absorbed oxygen. After oxidation, the peak at

532.9 eV for C–OH groups increase gradually, meaning that the main chemical groups introduced to the surface of graphene basal plane are hydroxyl groups during the electrochemical oxidation. A broad band at 534~530 eV is observed at the original G-P electrode without oxidation, which arises from the absorbed oxygen.

Fig. 6c and d show the high-resolution C1s and O1s of XPS spectra from the G-E and O 30 min-G-E electrodes, respectively. For the C1s spectra, there is a peak at 285.4 eV, compare to the original G-E electrode. That can be assigned to the peaks at 286.2 and 287.0 eV, corresponding to the C-OH, C=O species, respectively. The assignment of peaks in the O1s spectra for O 30 min-G-E is assign to ''carbon-oxygen'' functional groups. By comparing the C1s peaks, we have assigned the O1s peaks at 531.3 and 530.6 eV to the contribution from the C=O and O=C-OH groups, respectively. The O1s peak at 532.9 eV is assigned to the C-OH groups. There is an interesting phenomena. Notably, when compared the spectra O1s of O 30 min-G-P electrodes with that of O 30 min-G-E, the edge carbon atoms of graphite are much more inclined to be oxidized to carbon-oxygen double bond than that of basal plane atoms in the same electrochemical oxidation process.
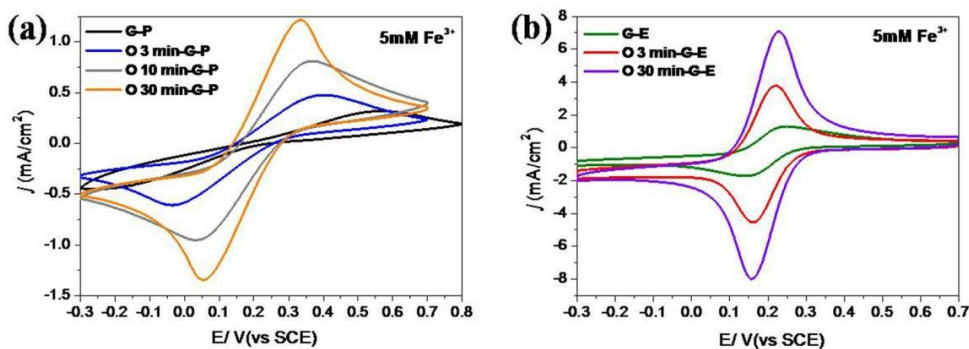
3.2. Carbon position (edge or basal plane) and oxidation state effects of graphene for biosensing

During the past twenty years, the popularity of nano/micro carbon such as carbon fiber, carbon nanotubes and graphene as electrode materials has increased dramatically.[22-25] The fact that these different types of carbon materials are commercially available has led to their use in a wide range of applications.[26, 27] However, despite the large amount of research conducted with carbon electrodes, there still remains uncertainty about the individual roles of the edge and basal-plane regions in the electrochemical response of a graphitic surface. Herein, $K_3[Fe(CN)_6]$, uric acid and ascorbic acid were used as probes to detect the electrochemical properties of the basal plane and edge atoms, and the effect of their oxidation state.
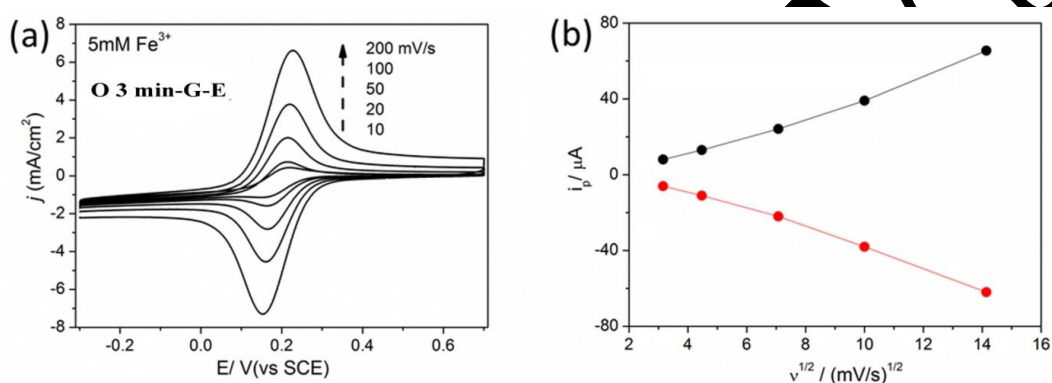
3.2.1 Electrochemical activity of $K_3[Fe(CN)_6]$ probe

Fig. 7 shows the cyclic voltammograms (CVs) of 5 mM $K_3[Fe(CN)_6]$ on the G-P and G-E electrodes with different oxidation times. In Fig. 7(a), the electrochemical oxidation caused some changes in the peak separation for the O-G-P electrodes (ΔEp≈690 mV for G-P and ΔEp≈280 mV for O 30 min-G-P), indicating that the electron-transfer kinetics is relevant to the oxygen species. In the meanwhile, different ΔEp values were observed for the O 3min-G-E (ΔEp ≈ 60 mV) and unoxidized (ΔEp ≈ 90 mV) electrodes under the same conditions (Fig. 7(b)). The decrease in ΔEp by 30 mV indicates an increased electron-transfer rate for the oxidized G-E electrode. Furthermore, the ΔEp of oxidized G-E electrode is close to 59 mV over the scan rates from 10 to 200 mV/s (Fig. 8(a)), which indicates a diffusion controlled Nernst process (in Fig. 8(b)).[28]

Figure 7. CVs of 5 mM $K_3[Fe(CN)_6]$ in 0.1 M PBS (pH 6.5) for the G-P (a) and G-E (b) electrodes with different oxidation time , at a scan rate of 100 mV/s
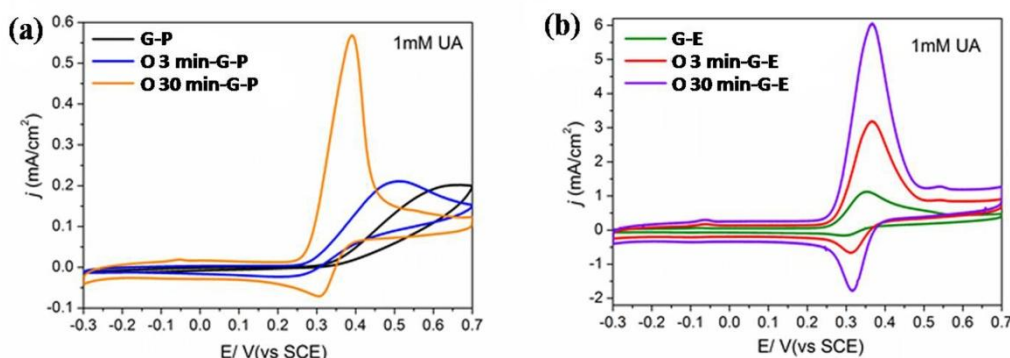

Figure 8. (a) CVs of 5 mM $K_3[Fe(CN)_6]$ in 0.1 M PBS (pH 6.5) at a scan rates scope of 10, 20, 50, 100 to 200 500 mV/s, (b) shows the relationship of plot of peak current and the square root of the scan rate.

Table 1. The oxidation and reduction peak potentials and currents of O-G-P and O-G-E electrodes with different oxidation time in CVs of 5 mMK$_3$[Fe(CN)$_6$].

	Epa (V)	Ipa (mA cm^{-2})	Epc(V)	Ipc (mA cm^{-2})	$\Delta E = E_{pa} - E_{pc}$ (mV)
G-P	0.54	0.18	-0.15	0.07	690
O 3 min-G-P	0.38	0.41	-0.03	0.37	410
O 10 min-G-P	0.33	1.08	0.05	0.85	280
G-E	0.24	1.4	0.15	1.3	90
O 3 min-G-E	0.22	3.7	0.16	3.3	60
O 10 min-G-E	0.23	6.9	0.16	6.6	70

3.2.2 Electrochemical activity of uric acid (UA)

Figure 9. Cyclic voltammograms of 1 mM UA recorded in 0.1 M PBS (pH 6.5) at a scan rate of 100 mV/s of the G-P (a) and G-E (b) electrodes with different oxidation time.

A summary of the oxidation and reduction peak potentials and currents of O-G-P and O-G-E electrodes with different oxidation time is shown in Table 1. The smaller values of ΔEp observed in the case of G-E and O-G-E electrodes indicates an enhanced electron-transfer rate at the edge electrodes (Fig. 7(b)). In addition the peak current of Fe^{3+} on the O-G-E electrodes increase significantly, which is attributed to the exfoliation of electrode surface that could be exposed more edge atoms as reactive sites.

Fig. 9 shows the cyclic voltammograms of 1 mM potassium UA at the G-P and G-E electrodes with different oxidation time. In Fig. 9(a), the electrochemical oxidation caused obvious changes obviously in the peak-to-peak separation of the O-G-P electrodes (no obvious peak at G-P and ΔEp≈ 80 mV for O 30 min-G-P, which is close to the idea potential difference of 59mV). Under the same conditions, in contrast, a constant ΔEp values of 60 mV was observed for the O-G-E and unoxidized electrodes under the same conditions (Fig. 9(b)).

Table 2. Summary of the oxidation and reduction peak potentials and currents at O-G-P and O-G-E electrodes with different oxidation time for cyclic voltammograms of UA.
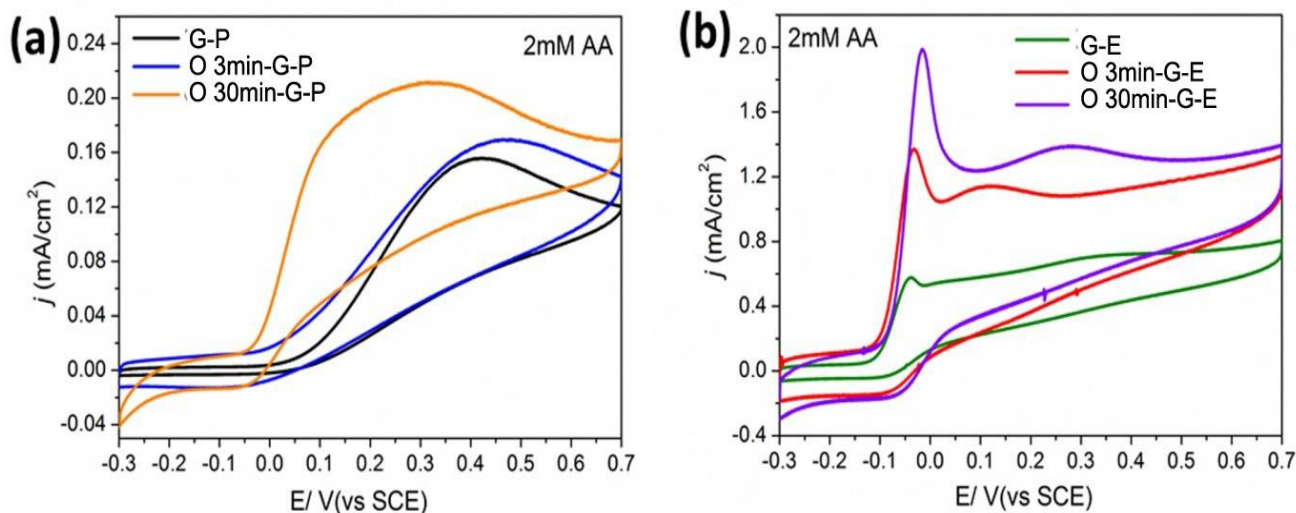
	Epa (V)	Ipa (mA cm^{-2})	Epc(V)	Ipc (mA cm^{-2})	ΔE= E_{pa}-E_{pc} (mV)
G-P	0.57	0.25	N	N	-
O 3 min-G-P	0.48	0.62	0.27	-0.2	210
O 30 min-G-P	0.39	2.59	0.31	-0.51	80
G-E	0.36	0.94	0.30	-0.15	60
O 3 min-G-E	0.36	2.82	0.30	-0.48	60
O 10 min-G-E	0.37	5.82	0.31	-1.44	60

N: No obvious peak

The oxidation and reduction peak potentials, currents of O-G-P and O-G-E electrodes with different oxidation times for CV detection of UA are shown in Table 2. A dramatic ΔEp change at the

O-G-E electrode was observed from 210 mV for 3 min oxidation to 80 mV for 30 min oxidation, which is more significant than the results from the above case of $K_3[Fe(CN)_6]$. This may be due to the oxygen and nitrogen groups in the UA molecular structure, which could interact with the oxygen groups (especially hydroxyl group) and be introduced to graphene basal plane. As a result, a further catalyst for the redox was obtained and also could enhance the electron-transfer rate reaction of UA.

3.2.3 Electrochemical activity of ascobic acid (AA)

Figure 10. Cyclic voltammograms of 2 mM AA recorded in 0.1 M PBS (pH 6.5) at a scan rate of 100mV/s of the G-P (a) and G-E (b) electrode with different oxidation time.

Fig. 10 shows the CV of ascorbic acid (AA, 2.0 mM) in 0.1 M PBS electrolyte (pH 6.5) at the G-P, G-E electrodes with and without oxidation. For the case of O 3min-G-E and O 30min-G-E elecrodes, there is no change in oxidation potential. For the O 3min-G-P and O 30min-G-P elecrodes, there is also no change in oxidation potential. The different Ep,a values for oxidation of AA were observed at the G-P and G-E electrodes, suggesting that the electron-transfer rate in AA varies greatly with the change of edge or basal carbon atoms' position but not with that of the oxygen groups.

4. CONCLUSIONS

In summary, the graphene basal plane and edge carbon atoms play a different role in electrochemistry at the graphene flak eelectrodes because of the used electrochemical species. The results demonstrated that the electrochemical oxidation induced oxygen-containing surface functionalities could regulate the electrochemical activities of graphene based electrode. According to the XPS results as direct evidences, the edge carbon atoms of graphite are much more inclined to be oxidized to the carbon-oxygen double bond. Nevertheless, in the electrochemical process, the main chemical groups that were introduced to the surface of graphene basal plane are hydroxyl groups.

The importance of carbon positions (the edge and basal plane sites of graphene) and oxygenated species in electroanalysis was highlighted. In electroanalysis, the control of the referred factors probably helps to the development of enhanced analytical sensors. For the electro-analyze of Fe^{3+} and UA, the response signal was sensitive to both the carbon position and oxidation state. For the case of AA, the redox reaction is only sensitive to carbon position, but not to oxidation state.

References

1. Y.Y. Shao, J. Wang, H. Wu, J. Liu, I.A. Aksay, Y.H. Lin, *Electroanal,* 22 (2010) 1027.
2. J.Y. Ji, Y. Li, W.C. Peng, G.L. Zhang, F.B. Zhang, X.B. Fan, *Adv Mater*, 27 (2015) 5264.
3. L. Fritea, M. Tertis, S. Cosnier, C. Cristea, R. Sandulescu, *Int. J. Electrochem. Sci.*, 10 (2015) 7292.
4. S. Gupta, M. vanMeveren, J. Jasinski, *Int. J. Electrochem. Sci.* 10 (2015) 10272.
5. L. Tang, Y. Wang, Y. Li, H. Feng, J. Lu, J. Li, *Advanced Functional Materials*, 19 (2009) 2782.
6. Y. Wang, Y.Y. Shao, D.W. Matson, J.H. Li, Y.H. Lin, *Acs Nano*, 4 (2010) 1790.
7. H. Shen, L.M. Zhang, M. Liu, Z.J. Zhang, *Nanoscale,* 2 (2012) 283.
8. Y. Wang, Y.M. Li, L.H. Tang, J. Lu, J.H. Li, *Electrochemistry Communications*, 11 (2009) 889.
9. R.K. Srivastava, S. Srivastava, T.N. Narayanan, B.D. Mahlotra, R. Vajtai, P.M. Ajayan, A. Srivastava, *Acs Nano*, 6 (2012) 168.
10. T. Xue, S. Jiang, Y. Qu, Q. Su, R. Cheng, S. Dubin, C.-Y. Chiu, R. Kaner, Y. Huang, X. Duan, *Angewandte Chemie International Edition,* 51 (2012) 3822.
11. L.H. Tang, Y. Wang, J. Liu, J. Li, *Acs Nano*, 5 (2011) 3817.
12. M. Pumera, *The Chemical Record,* 9 (2009) 211.
13. T.J. Davies, M.E. Hyde, R.G. Compton, *Angewandte Chemie*, 117 (2005) 5251.
14. A. Chou, T. Böcking, N.K. Singh, J.J. Gooding, *Chem. Commun.*, (2005) 842.
15. X.B. Ji, C.E. Banks, A. Crossley, R.G. Compton, *Chemphyschem*, 7 (2006) 1337.
16. M.M.I. Khan, A.M.J. Hague, K. Kim, *J. Electroanal. Chem.*, 700 (2013) 54.
17. C.A. Goss, J.C. Brumfield, E.A. Irene, R.W. Murray, *Analytical chemistry*, 65 (1993) 1378.
18. Z.Y. Xia, S. Pezzini, E. Treossi, G. Giambastiani, F. Corticelli, V. Morandi, A. Zanelli, V. Bellani, V. Palermo, *Advanced Functional Materials*, 23 (2013) 4684.
19. G.D. Ewen Smith, Modern Raman spectroscopy- a practical approach, 2004.
20. Z. Ni, Y. Wang, T. Yu, Z. Shen, *Nano Res,* 1 (2008) 273.
21. C.H. An Wong, A. Ambrosi, M. Pumera, *Nanoscale,* 4 (2012) 4972.
22. X. Li, B.Q. Wei, *Nano Energy*, 2 (2013) 159.
23. R.L. McCreery, *Chem Rev*, 108 (2008) 2646.
24. H. N. A. Mustafa, I. M. Isa, N. M. Ali, N. Hashim, M. Musa, S. Ab Ghani, *Int. J. Electrochem. Sci.,* 10 (2015) 9232.
25. B. S. He, J. X. Zhang, *Int. J. Electrochem. Sci.,* 10 (2015) 9621.
26. A.K. Geim, K.S. Novoselov, *Nat Mater*, 6 (2007) 183.
27. Zaidi, S. A. *Int. J. Electrochem. Sci.*, 8 (2013) 11337.

28. R.L. McCreery, In Electroanalytical Chemistry, in: A.J. Bard (Ed.), Dekker, New York, 1991, pp. 221-374.